3 Molecular Crystal Project

– Precise crystal structure analysis for investigating the origin of physical properties in molecular crystals –

Project Leader: Reiji Kumai

In this project, electronic correlation in molecular crystal systems is being investigated to elucidate novel phenomena such as superconductivity and charge ordering. We will analyze crystal structures of molecular crystals under high pressure and/or at low temperature to elucidate the origins of phase transitions.

3-1 Structure–property relationship of supramolecular ferroelectric [H-66dmbp][Hca] accompanied by high polarization, competing structural phases, and polymorphs [1]

Ferroelectricity is a key issue in condensed matter physics. In ferroelectric materials, the application of an external electric field, E, can switch the spontaneous polarization through the inverting polarity of the noncentrosymmetric crystal structure. By making use of such property, ferroelectric materials can be applied in various electric applications such as memory, sensor, actuator, and optical devices. Most of these devices are made from inorganic ferroelectrics such as Pb(Ti,Zr)O_3 (PZT), SrBi$_2$Ta$_2$O$_9$, BaTiO$_3$, and LiNbO$_3$ because their operation in ambient environments demands a large spontaneous polarization (P_s) and high Curie temperature (T_C) of a paraelectric-to-ferroelectric phase transition near or above room temperature.

Recently, organic ferroelectric materials containing neither toxic nor rare elements have attracted significant attention due to their flexible, environmentally friendly, fusible, and low-cost characteristics. Specifically, single-component hydrogen-bonded compounds such as croconic acid and benzimidazoles have led to a significant improvement in the P_s and T_C up to far above room temperature. The structural

and electronic mechanisms of ferroelectricity in this organic system can involve intramolecular and intermolecular processes, and can lead to characteristics distinct from those of inorganic ionic ferroelectrics. Structural characterizations are indispensable for understanding the microscopic mechanism of ferroelectricity, which may be useful for advancing the design of various materials. For instance, X-ray diffraction studies on poled crystals of tetrathiafulvalene (TTF)-p-chloranil (CA) complex revealed that unexpectedly large electric polarization originates from intermolecular charge-transfer processes and consequently is directed antiparallel to the static charge (ionic) displacement.

In this study, we examined the structure–property relationship of ferroelectric binary-compound crystals, in which hydrogen-bonding forms a one-dimensional supramolecular chain of alternating acid and base molecules. Using a series of anilic acids, the polarity of the proton-transferred monovalent ionic form can be switched through collective proton transfer between neighboring acid and base molecules. Many of these supramolecular crystals undergo structural phase transitions related to proton order-disorder phenomena.

As compared to the aforementioned single component materials, ferroelectric supramolecules were reported to exhibit modest T_C and P_s until recent findings regarding 6,6′-dimethyl-2,2′-bipyridinium chloranilate [H-66dmbp][Hca] (Fig. 1). This compound, which has the longest hydrogen bond length among organic ferroelectric supramolecules, was first reported by Bator *et al.*[2] A spontaneous polarization P_s of 7–8 μC cm^{-2} was about half of that of croconic acid (~21 μC cm^{-2}) and comparable to that (~10 μC cm^{-2}) of
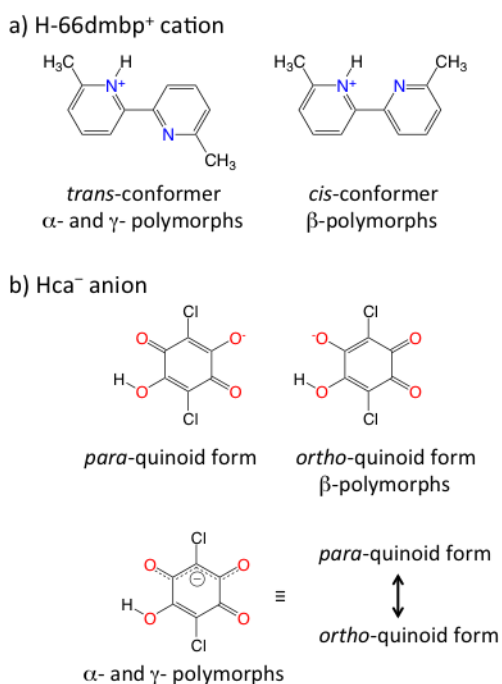
Fig. 1: Chemical structures of (a) the different conformations of bipyridinium and (b) the π-bond geometries of chloranilate in the three polymorphs of [H-66dmbp][Hca] salt.

benzimidazoles and ferroelectric polymers such as poly(vinylidene fluoride) (PVDF) and its copolymer with trifluoroethylene (TrFE). Here, we highlight the dielectric and structural properties of [H-66dmbp][Hca] in order to understand the origin of the large P_s and thermally robust ferroelectric phase persisting up to ~380 K. Comparison with other supramolecular crystals with varying hydrogen-bond parameters enabled the establishment of structural design principles for improved electric and thermal properties.

[H-66dmbp][Hca] was obtained from a solution of a 1:1 stoichiometric mixture of 66dmbp and H_2ca. In addition to the ferroelectric (α-) form, X-ray crystal structure analysis revealed two additional polymorphs, called the β- and γ- form hereafter, obtained under different crystallization conditions (see the experimental section for details). The color of the α-form (elongated plates), β-form (polygons), and γ-form (blocks) crystals was dark red. The polymorphs could be distinguished from one another by infrared spectra, the molecular conformations of H-66dmbp$^+$ (cis- or trans-form), and/or π-bond geometry of Hca$^-$ (resonant hybrid or ortho-quinoid form) (Fig. 1).

The measurement of dielectric constants is typically a suitable way to identify phase transition points, especially the Curie temperature, of

ferroelectrics. The ferroelectric a-form exhibited a discontinuous jump at 382 K (or 366 K) in the heating (or cooling) process, as shown in Fig. 2a. The observed thermal hysteresis manifested a first-order phase transition and was consistent with the differential scanning calorimetry (DSC) measurements. This phase transition corresponded to the disappearance of the ferroelectric state, as confirmed by the sudden collapse of the *P-E* hysteresis loops (inset to Fig. 2a), as well as by previous pyroelectric current measurements, which demonstrated the disappearance of the large spontaneous polarization above this temperature. Notably, the temperature dependence of the dielectric constant did not obey the Curie-Weiss law. A rounded peak anomaly of permittivity was also noted at 320 K in the cooling process, and its appearance and amplitude strongly depended on the applied frequency and specimen. It was not accompanied by endothermic/exothermic anomalies in DSC. These features signified an extrinsic origin, such as domain-wall motion, as opposed to a phase transition. The a-form crystal exhibited a melting point at 453 K and underwent thermal decomposition just above this temperature as shown by the exothermic peak with rapid weight loss in the thermogravimetric and differential thermal analysis (TG-DTA).
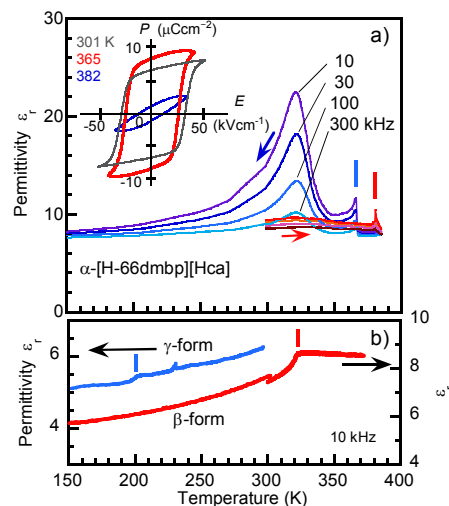

Fig. 2: Temperature dependence of the relative permittivity *e*r of [H-66dmbp][Hca] single crystals. (a) Ferroelectric α-form measured with the ac field applied along the hydrogen-bonded chain (parallel to the crystallographic *b*-direction). (b) Non-ferroelectric β- and γ-forms with the ac electric field applied along the crystal [1-1-1] and [2-10] directions, respectively. Inset: Variation of electric polarization (*P*) – electric field (*E*) hysteresis loops of the α-form crystal (*E*//*b*, *f* = 30 Hz) upon cooling.

The β- and γ- crystal forms exhibited a relative permittivity of less than 10 and a temperature dependence that was distinct from that of the a-form (Fig. 2b). We found a small kink-like anomaly at 322 K in the dielectric constant in addition to a couple of endothermic and exothermic peaks in DSC for the β-form. The dielectric and thermal properties indicative of the phase transition were in agreement with the report by Bator et al.[2] The γ-form crystal showed a tiny kink anomaly at 201 K on the nearly flat ε_r-T curve. These anomalies were identified as phase transitions, and were accompanied by a pair of endothermic and exothermic peaks in the DSC measurements, which signified an additional first-order phase transition around 370 K.

Based on the aforementioned experimental results, we concluded that the findings of Bator et al. could be ascribed to the properties of the β-form crystal, with the exception of the crystal structure of the α-form. Each crystal form exhibits two or three different structural phases, which will be distinguished hereafter as phases I, II, and III from the low-temperature side with a subscript specifying the polymorph. For instance, the phase Ia corresponds to the ferroelectric state.

The crystal structure of [H-66dmbp][Hca] was previously reported only for the α-form. The H-66dmbp$^+$ cation adopts the trans conformation. The intramolecular bond lengths of the Hca$^-$ anion indicate the resonance hybrid of para- and ortho-quinoid geometries. These cations and anions form individual π-stacked columns parallel to the a-axis. At room temperature (phase Ia), the crystal structure belongs to the monoclinic system with the non-centrosymmetric and polar space group $P2_1$. Importantly, the overall crystal structure exhibited the pseudo-symmetric character of space group $P2_1/c$, whereas the dominant origin of polarity was the asymmetric proton location. These features are promising for the simple reversal of polarization. To investigate the structural changes between the Ia and IIa phases, the crystal structure was determined at room temperature (T = 300 K) and T = 375 K (in the temperature hysteresis range after heating to 390 K).

In the ferroelectric (FE) phase Ia (T = 300 K) structure, H-66dmbp and Hca exhibited an almost planar molecular geometry. They were alternately linked with a large dihedral angle of 79.9° through the OH⋯N or N$^+$H⋯O$^-$ bonds, forming a linear supramolecular chain. All protons between H-66dmbp and Hca were uniformly ordered in the hydrogen-bonded chain. Because the polarities of the chains were aligned in the crystallographic b-direction, the spontaneous polarization appeared along this direction, as shown in Fig. 3a.

α-[H-66dmbp][Hca] had the longest hydrogen-bonding length (d_{O-N} = 2.95 Å) among the acid-base type supramolecular ferroelectrics. The hydrogen bond was accompanied by intermolecular CH⋯O interactions with the methyl group and pyridine ring of the same H-66dmbp molecule. The H⋯O distances of 2.49 Å and 2.34 Å were shorter than the sum of the van der Waals radii (2.72 Å) of the hydrogen and oxygen atoms, and prevented further shortening of the hydrogen bonds by steric hindrance.

The high-temperature phase IIa (T = 375 K) exhibited superlattice reflections indicative of unit-cell doubling. The new unit-cell was related by (**a'**, **b'**, **c'**) = (2**a**, **b**, **c** - **a**) (Fig. 3b). In the transformation to phase IIa, the twist angle of H-66dmbp at the central C=C bond increased from 2.9° to 8.0°, and the dihedral angle between H-66dmbp and Hca decreased by about 1°. Notably, all protons were ordered in the OH⋯N and N$^+$H⋯O$^-$ bonds, and each supramolecular chain maintained the polar nature. The space group is centrosymmetric $P2_1/c$ and an inversion center appeared in the intermolecular space. The polarity of the chains alternated along the doubled a-direction in the antipolar
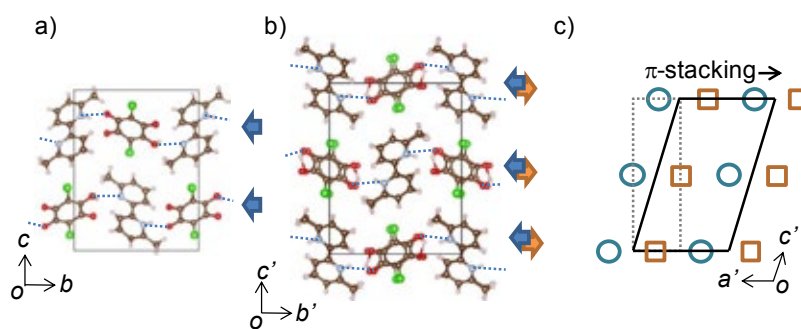

Fig. 3: Crystal structures of α-[H-66dmbp][Hca] in (a) phase Ia (T = 300 K) and (b) phase IIa (375 K). Blue and red arrows indicate polarity of hydrogen-bonding chains. (c) Schematic drawing of cell transformation of high-temperature structure viewed along the direction of the hydrogen bond. Dotted gray and solid black lines show the unit-cell at room temperature and high temperature, respectively.

(antiferroelectric (AFE)-type) structure (Fig. 3c). This finding indicated that the interchain dipole-dipole interactions created a similar stability of the FE and AFE structures, suitable for interchange even with the change in temperature. This FE-AFE type structural change has not been observed for other hydrogen-bonded organic compounds, but was reported for a pressure-induced phase transition in a CsH_2PO_4 (CDP) crystal.

As shown in Fig. 4a, the hydrogen bond length <*d*> ranged from 2.57–2.70 Å and the phase transition temperature increased with increasing <*d*>, with the exception of the α-[H-66dmbp][Hca] crystal (the orange star). The observed positive correlation between T_C and <*d*> was similar to that of KH_2PO_4 (KDP) type ferroelectrics, in which the thermal stability of ferroelectricity is described by the off-centering of protons: the contraction of the distance between two equilibrium positions of protons decreases the potential barrier and then destabilizes the ferroelectric state. This is corroborated by the fact that ferroelectric [H-55dmbp][Hia] exhibited a decreased Curie temperature T_C with the application of hydrostatic pressure. By assuming a linear relationship, the longest <*d*> (2.88 Å) corresponded to a Curie temperature of about 600 K for the α-[H-66dmbp][Hca] crystal. However, the actual phase transition temperature (378 K) was much lower than the extrapolated value and suggested a distinct structural origin for the disappearance of spontaneous polarization. The ferroelectric state of α-[H-66dmbp][Hca] was found to change into the AFE structural phase before the thermal activation moved the protons toward disordered or centered locations in the hydrogen bond. The proton-ordered state (AFE phase) persists up to the melting point at 453 K. Despite the emergence of this competing phase, the thermal stability of the ferroelectric phase was suitable for the stretched hydrogen bonds of the α-[H-66dmbp][Hca] crystal.

A positive correlation between P_s and <*d*> (Fig. 4b) was also found. For further understanding, the total polarization ($\mathbf{P}^{calc}$) of supramolecular ferroelectrics was also evaluated theoretically using first-principles electronic structure calculations with the Berry phase technique for the three supramolecular ferroelectrics, a-[H-66dmbp][Hca], [H-dppz][Hca], and [H-55dmbp][Hia]. We used computationally optimized hydrogen positions when stating the X-ray diffraction data, which tend to underestimate the C–H bond lengths. The
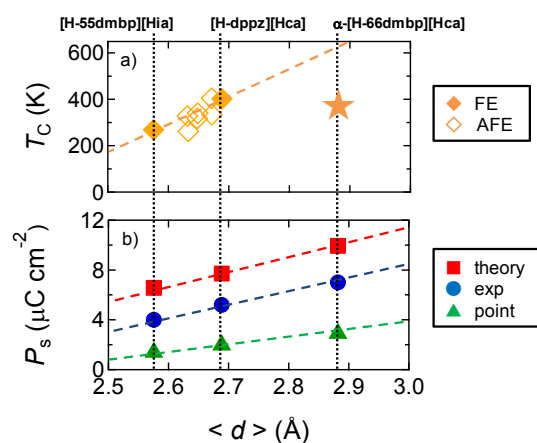

Fig. 4: Ferroelectric properties of acid-base supramolecular crystals plotted as a function of hydrogen bond distance <*d*>. (a) Phase transition temperature (T_C). The orange star indicates the FE-to-AFE phase transition point of α-[H-66dmbp][Hca]. (b) Spontaneous polarization (P_s) of ferroelectric compounds. Red squares, blue circles, and green triangles show the theoretical values obtained from first-principles calculations, experimental values, and point-charge-model estimates, respectively.

polarizations exhibited good agreement with the theoretical and experimental data and exhibited a linear relationship with <*d*>.

In the ferroelectric compounds, the spontaneous polarization was nearly parallel to the direction of the proton transfer from the nitrogen to oxygen atom (or vice versa). One can easily imagine that P_s can be increased by separating the two equilibrium positions with increasing <*d*>. For simplicity, the ionic polarization $\mathbf{P}^{ion}$ was roughly estimated under the point-charge approximation:

$$\mathbf{P}^{ion} = \Sigma_{(cell)} Z_i |e| \mathbf{u}_i / W$$

where e is the electron charge and W is the unit-cell volume.

$\mathbf{P}^{ion}$ was calculated from the relative displacement $\mathbf{u}_i$ of static molecular (or proton) charges $Z_i|e|$. The point charges were placed on the proton, base, and chloranilate (ca^{2-}) cores as Z_i = +1, 0, and –2, respectively. The ca^{2-} core was put on the center of gravity of the six-membered ring, whereas the protons were defined in the same positions as those used for the aforementioned theoretical calculations. The $\mathbf{u}_i$ of each point charge is the displacement from the corresponding paraelectric structure, which was constructed by imposing an inversion symmetry on the ferroelectric structure. The calculated $\mathbf{P}^{ion}$ actually increased with <*d*> as expected, and was about half of the experimental P_s. It was considered that the rest of the polarization originated from the charge
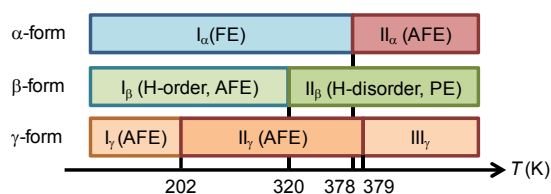
Fig. 5: Phase transition sequences of three [H-66dmbp][Hca] polymorphs. The transition temperatures represent those determined by the endothermic peak in the first heating run.

density modulation within the molecules, which was completely neglected in the point-charge model. This fact highlights the significant role of the p-electron system in electric polarization.

The β- and γ- polymorphs also show some structural phase transitions, which are summarized in Fig. 5. The hydrogen bonds in the β-form crystal undergo a proton-disordered state near room temperature (i.e. the II_b phase), but the α- and γ-polymorphs exhibit the thermally robust nature of the proton-ordered state, including ferroelectric structure. The improved stability of the polar chain in the latter polymorphs can be related to the significantly elongated O···N distance, because the *trans* conformer of H-66dmbp$^+$ enhances the steric hindrance around the hydrogen bond, in contrast to the case of *cis* conformer. These two polymorphs are also similar in terms of the phase transition, which reorganizes the interchain configuration of parallel or antiparallel polarities. The major difference between the a- and g- polymorphs is the presence or absence of the ferroelectric state, although the only apparent structural difference was the axial orientation of the *trans* H-66dmbp$^+$, which was alternating (along the [011] direction) in the α-polymorph, but uniform in the γ-polymorph. These observations suggested that ferroelectric and antiferroelectric-type interactions were competing among the polar chains to reveal a variety of polar and antipolar structural motifs. It should be noted that conformational changes of H-66dmbp$^+$ play an important role in the polymorphism and structural phase transitions of the polymorphs. Specifically, the rich variety of structural phases in [H-66dmbp][Hca] is the consequence of the flexibility and small *trans*/*cis* interconversion energy of the 2,2′-bipyridine unit.

We have investigated the structure–property relationship of [H-66dmbp][Hca] polymorphs as well as some related supramolecular crystals in order to understand the origin of polarization and the thermally stable ferroelectricity of the a-form crystal. The flexible *trans*/*cis* interconversion of the H-66dmbp cation was responsible for the formation of the polymorphs and their various structural phases.

A positive relationship between the phase transition temperature T_c and the hydrogen bonding distance <d> was observed for the proton off-centering or order-disorder phenomena. The thermal stability of the ferroelectric or antiferroelectric state was related to the potential barrier height of the off-centered protons. Although the increase in <d> due to the steric hindrance of the *trans* conformer of H-66dmbp partly explained the high-temperature ferroelectricity of α-[H-66dmbp][Hca] up to 378 K, this upper limit was much lower than the expected temperature (~600 K). For this reason, the crystal structure analysis at 375 K revealed a structural phase transition from the ferroelectric to antiferroelectric ordered state. The phase transition changed significantly with the twist angle of *trans* H-66dmbp, as was also seen in the γ-polymorph.

The optimized spontaneous polarization P_s in the measurements agreed well with the results of first-principles calculations, and clearly showed a positive correlation with <d>. This observation was partly explained by the point-charge picture, in which P_s can be increased by separating the two equilibrium positions of protons with increasing <d>. On the other hand, the contribution from the altered intramolecular π-electron distribution, which is discarded in the point-charge model, exceeded half of the total polarization. This fact indicated that the large P_s of supramolecular ferroelectrics constitutes the cooperative effect of proton and p-electron dynamics. In summary, the experimental and theoretical data consistently demonstrated that stretching the hydrogen bond distance is a promising way to enhance the polarization performance and thermal stability of hydrogen-bonded organic ferroelectrics.

References
[1] K. Kobayashi, S. Horiuchi, S. Ishibashi, F. Kagawa, Y. Murakami, and R. Kumai, *Chem. Eur. J.* **2014** *20*, 17515.
[2] G. Bator, W. Sawka-Dobrowolska, L. Sobczyk, E. Grech, J. Nowicka-Scheibe, A. Pawlukojć, J. Wuttke, J. Baran, and M. Owczarek, *J. Chem. Phys.* **2011**, *135*, 044509.